CHAPTER (IV)

RELATIONSHIPS AND CLASSIFICATION

CHAPTER 4
RELATIONSHIPS AND CLASSIFICATION

Petrophysical relations are used for the interpretation of data of exploration geophysics, well logging, engineering, mining and environmental geophysics. Moreover, petrophysics is a cornerstone and magic key for solving geophysical problems and introducing theories. Therefore, the study of rock physics provides an interdisciplinary concept and tools that can facilitate and enhance geophysical interpretation. It is the main objective of this thesis to reveal relationships between different petrophysical parameters. The petrophysical investigation of directional parameters has confirmed that in general the laminated samples show a distinct anisotropy. The relations between parameters characterizing the anisotropy of different petrophysical should be investigated in detail.

4-1. Bulk density - porosity relationship

The bulk density - porosity relationship for the studied samples is shown in Figs. 4-1, 2. An inverse relationship is shown characterized by a coefficient of determination for all, laminated and non-laminated samples of 0.83, 0.75 and 0.81, respectively. The data is compiled in Tables 2-1, 2, 3 of appendix 1.

The bulk density - porosity relationship in Fig 4-1, 2 controlled by the following equations:

for all samples

$$\Phi = 0.847 - 0.318\, d_b, \qquad (1)$$

for laminated samples

$$\Phi = 0.713 - 0.262\, d_b, \qquad (2)$$

and for or non-laminated samples:

$$\Phi = 0.930 - 0.351\, d_b. \qquad (3)$$

with the bulk density given in g/cm^3 and the porosity as fractional value.

Regarding the mixing law for bulk density

$$d_b = (1-\Phi)d_g + \Phi d_f$$

and considering that the density of the fluid becomes negligible for dry samples ($d_f \approx 0.0 g/cm^3$), the porosity Φ can be determined by the following formula:

$$\Phi = 1 - \frac{d_b}{d_g}. \qquad (4)$$

If the grain density of quartz is considered (d_g = 2.65 g/cm³) for sandstone samples equation 4 provides a good porosity approximation. It can be noticed that the non-laminated samples follow the theoretical equation. The laminated samples show a larger scatter.

4-2. Bulk density – magnetic susceptibility relationship

The bulk density - susceptibility cross plot for the Bahariya samples is shown in Figs. 4-3, 4. The data points are highly scatted. The relationship is characterized only by a weak coefficient of determination of 0.35. The figure indicates a positive trend with an increasing of magnetic susceptibility with increasing bulk density.

The non-laminated samples are characterized by a low magnetic susceptibility and low variation in bulk density. It can be noticed that the lower left quarter in Fig. 4-4 contains only non-laminated samples having low magnetic susceptibility and bulk densities less than 2.38 g/cm³ while the upper right quarter is filled only with laminated samples with high magnetic susceptibility and higher bulk density. The lower right quarter remains empty while the upper left quarter contains non-laminated samples wit high magnetic susceptibility and laminated samples with bulk density less than 2.38 g/cm³. The data is listed in Tables 2-1, 2, 3 of appendix 1.

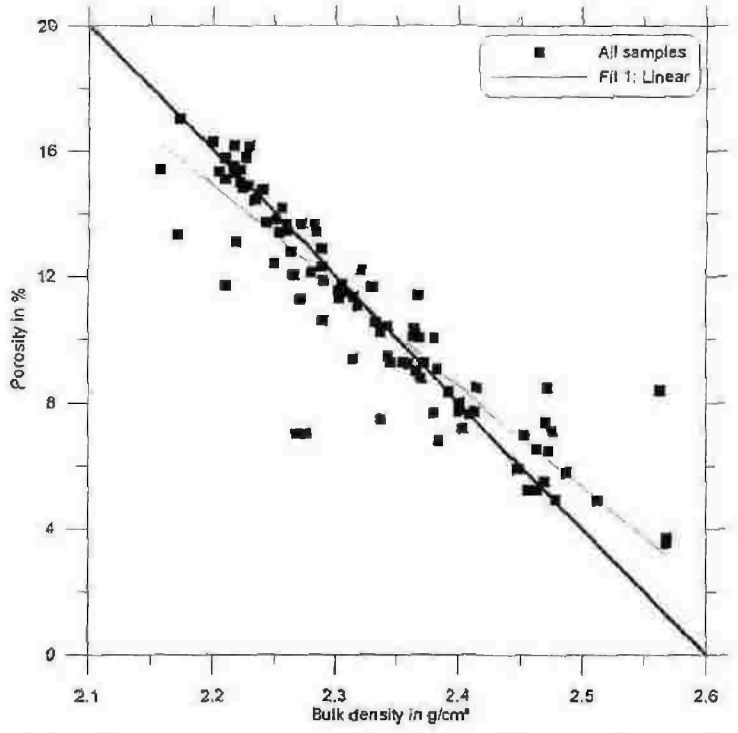

Fig.4-1 Bulk density versus porosity for all samples of the Bahariya Formation. 94 data points are used.

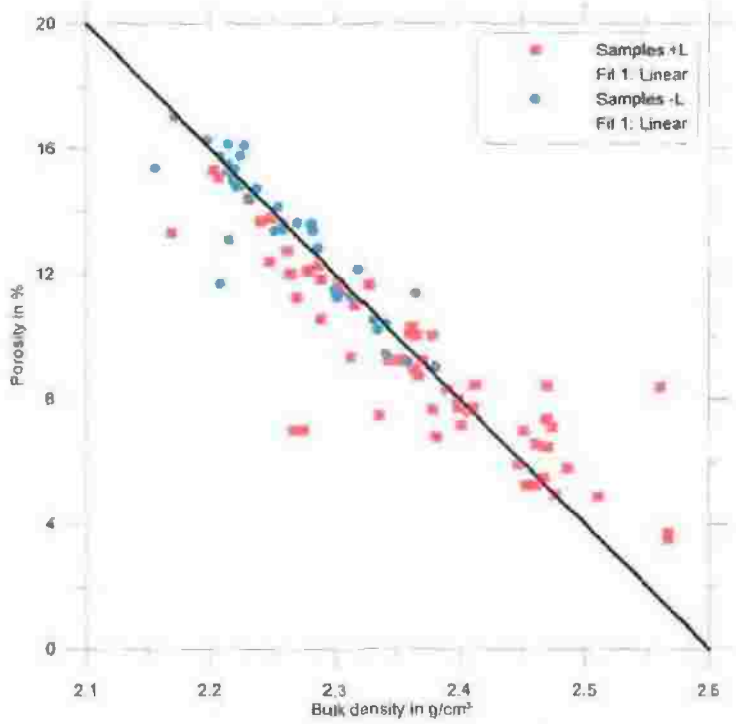

Fig.4-2 Bulk density versus porosity for laminated and non-laminated samples of the Bahariya Formation. 56 data points are used for laminated samples and 38 data points are used for non-laminated samples.

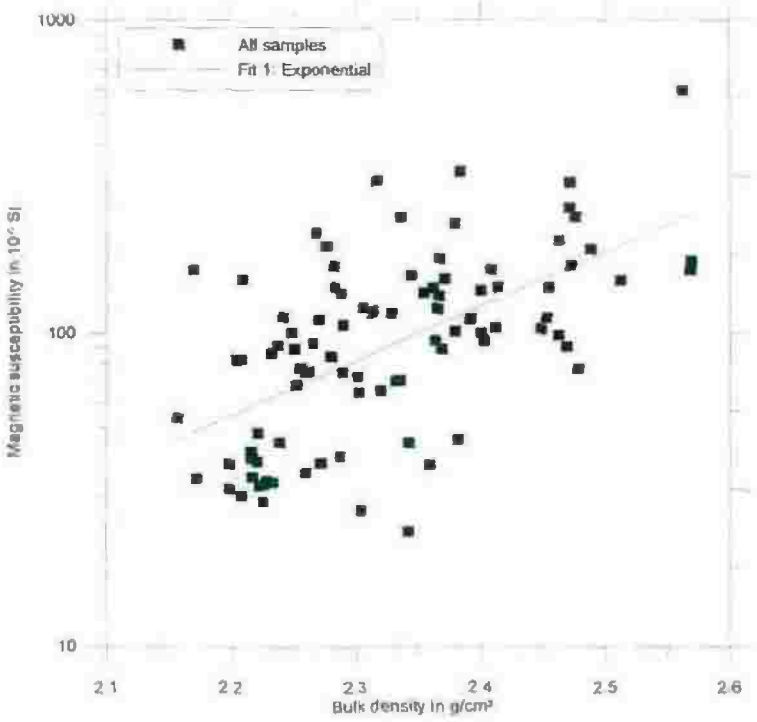

Fig. 4-3 Bulk density versus magnetic susceptibility for all samples of the Bahariya Formation. 94 data points are used.

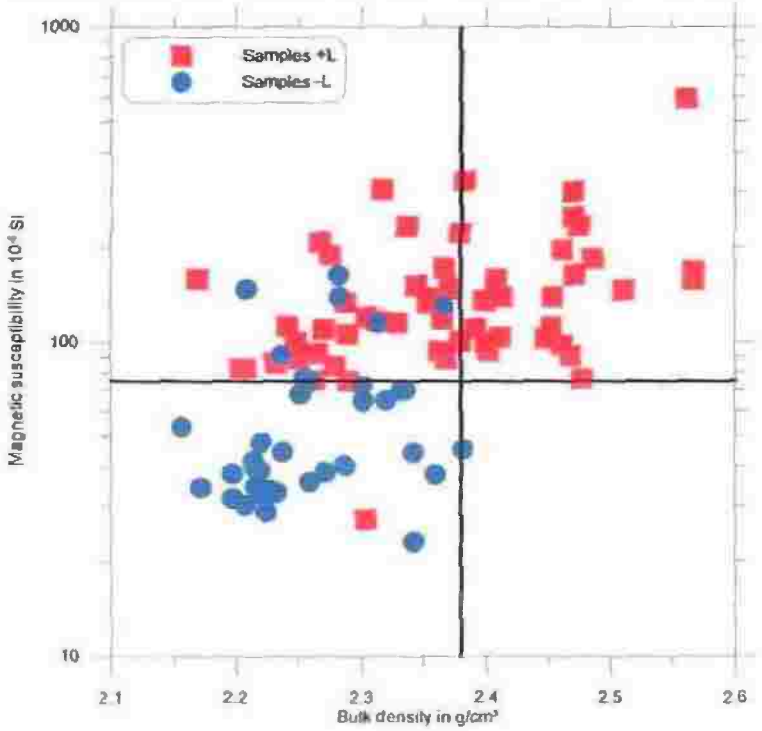

Fig. 4-4 Bulk density versus magnetic susceptibility for laminated and non-laminated samples of the Bahariya Formation. 56 data points are used for laminated samples and 38 data points are used for non-laminated samples.

4-3. Permeability - porosity relationship

The permeability of a rock may be affected by many geological factors. High rock porosity does not guarantee that a significant permeability exists. The pores must be interconnected, and the porethroats must be large enough to permit the flow of fluids. Pumice stone and shale are characterized by a very high porosity but very low permeability. On the other hand, micro fractured carbonates show low porosity but high permeability. A pore network is made up of larger spaces that are referred to as pores, which are connected by small spaces referred to as pore throats. In other words, the volume of pore space is reflected by the measured porosity, while the size of pore throats is reflected by the measured permeability of a rock. The geometric relationship between pore spaces and pore throats controls the relationship between porosity and permeability. The relationship between porosity and permeability has been studied by many authors, e.g. **Carman (1937), Timur (1968), Scheidegger (1974), El Sayed (1981), Herron (1987), Adler et al. (1990), Schön, (1996),** and **Tiab and Donaldson (2004).**

In the present work, porosity – log permeability cross plots exhibiting the investigated samples are shown in Figs. 4-5, 6. The data points in these figures follow the expected positive trend between porosity and permeability characterized by coefficients of determination for all, laminated and non-laminated samples of 0.63, 0.31 and 0.54, respectively.

The porosity - log permeability relationship is controlled by the equations:

for all samples:

$$k = [10]^{(0.27\,\Phi - 3.14)}, \quad (5)$$

for laminated samples:

$$k = [10]^{(0.16\,\Phi - 2.35)}, \quad (6)$$

and for non-laminated samples:

$$k = [10]^{(0.24\,\Phi - 2.47)}. \quad (7)$$

The porosity - log permeability cross plot for horizontal and vertical samples is shown in Fig. 4-7. The resulting correlations shown in these figures are characterized by coefficients of determinations for horizontal and vertical samples of 0.64 and 0.72, respectively. The porosity - log permeability relationships for horizontal and vertical samples are controlled by the following equations:

for horizontal samples:

$$k = [10]^{(0.24\,\Phi - 2.54)}, \quad (8)$$

find for vertical samples:

$$k = [10]^{(0.31\,\Phi - 3.87)}. \quad (9)$$

The laminated samples show generally lower porosity and permeability than the non-laminated samples. The layering in laminated samples filled by clay minerals that cause a decrease in porosity and permeability. The results of porosity and permeability determination of the studied samples are listed in Tables 2-1, 2, 3 of appendix 1 and Tables 3-1, 2, 3 of appendix 2.

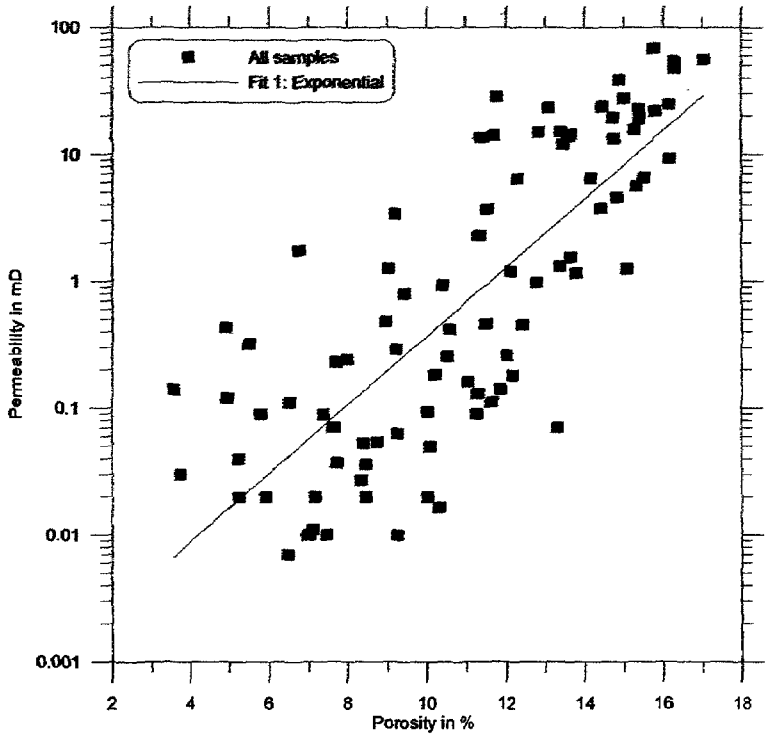

Fig. 4-5 Porosity versus logarithm of permeability for all samples of the Bahariya Formation. 92 data points are used.

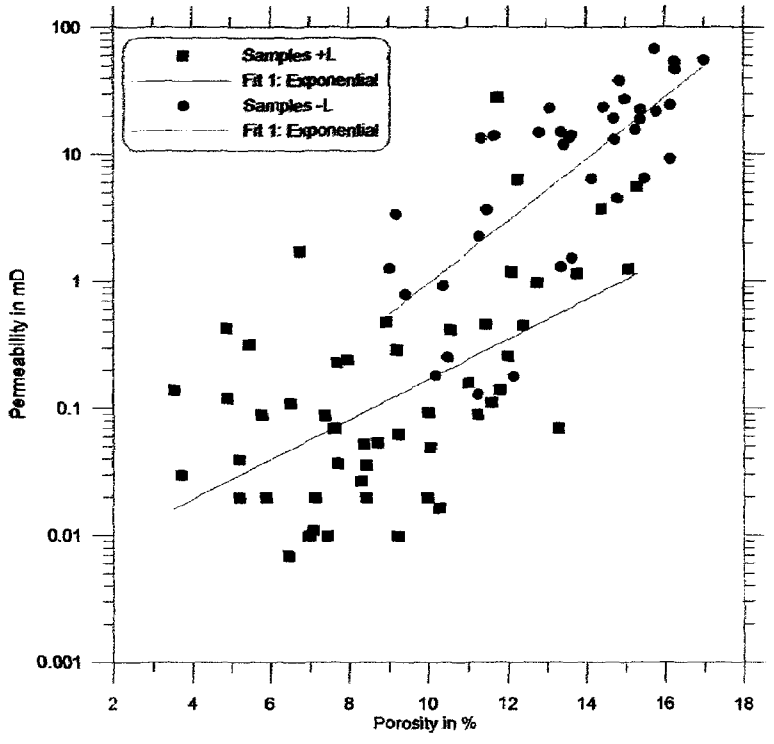

Fig. 4-6 Porosity versus logarithm of permeability for laminated and non-laminated samples of the Bahariya Formation. 54 data points are used for laminated samples and 38 data points are used non-laminated samples.

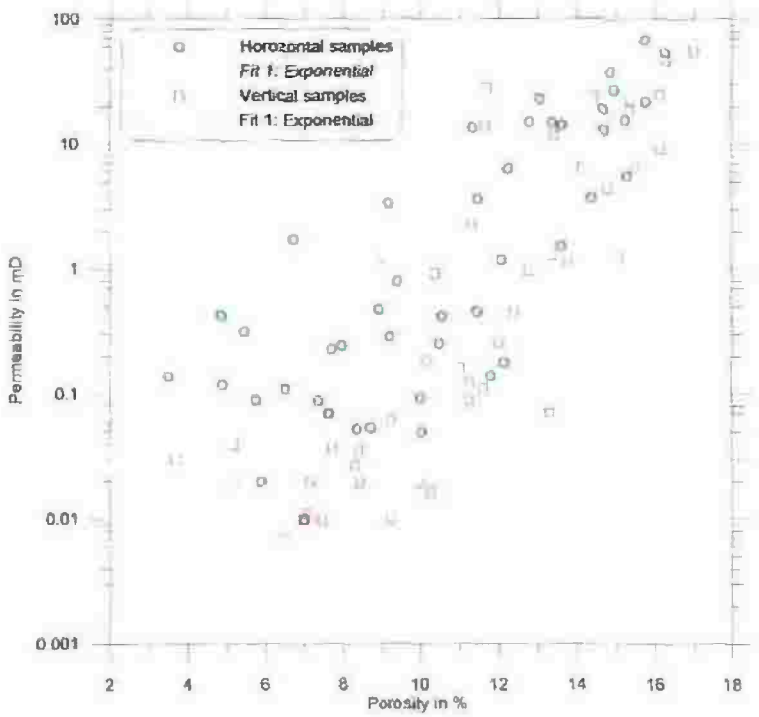

Fig. 4-7 Porosity versus logarithm of permeability for horizontal and vertical samples of the Bahariya Formation. 45 data points are used for horizontal samples and 47 data points are used for vertical samples.

4-4. Magnetic susceptibility – porosity relationship

The magnetic susceptibility - porosity cross plot for the Bahariya samples is shown in Fig. 4-8. The resulting correlations results in a coefficient of determination for all samples of 0.38. The susceptibility - porosity relationship shows a negative trend with an increase of porosity with decreasing magnetic susceptibility for all samples, which is controlled by the equation

$$\Phi = 25.18 - 7.31\ \kappa. \qquad (10)$$

The cross plot in Figure 4-9 summarizes the effects of lamination on porosity and magnetic susceptibility. These two parameters, which show the most significant effect amongst scalar parameters, can be used for a rough classification. The non-laminated samples generally show lower magnetic susceptibility and higher porosity. It can be noticed that the lower right quarter in Fig. 4-9, contains only laminated samples while the lower left quarter remains empty. The upper left quarter contains only non-laminated samples with high porosity and low magnetic susceptibility. The upper right quarter is filled with non-laminated samples with higher magnetic susceptibility and laminated samples with

porosity larger than 9%. The data is listed in Tables 2-1, 2, 3 of appendix 1. Generally, the non-laminated samples have higher porosity and lower susceptibility. The laminated samples show higher magnetic susceptibility due to the presence of a certain amount of iron minerals that cause an increased magnetic susceptibility.

4-5. Magnetic susceptibility – permeability relationship

The magnetic susceptibility - permeability cross plot for the Bahariya samples is shown in Fig. 4-10. The resulting correlation is characterized by a coefficient of determination for all samples of 0.48.

The susceptibility - permeability relationship shows a general increase of permeability with decreasing magnetic susceptibility for all samples which is controlled by the equation:

$$k = [10]^{(5.21)} * [\kappa]^{(-2.77)}. \qquad (11)$$

The susceptibility - permeability cross plot for laminated and non-laminated samples is shown in Figs. 4-11. It can be noticed that upper left quarter contains only non-laminated samples with high permeability and low magnetic susceptibility. The lower right quarter is filled with laminated samples and non-laminated samples with permeability less than 0.7 mD. The upper right quarter is filled with laminated samples with permeability larger than 0.7 mD and non-laminated samples with higher magnetic susceptibility while the lower left quarter remains empty. Generally, the non-laminated samples show higher permeability and lower magnetic susceptibility. The data is listed in Tables 2-1, 2, 3 of appendix 1 and Tables 3-1, 2, 3 of appendix 2.

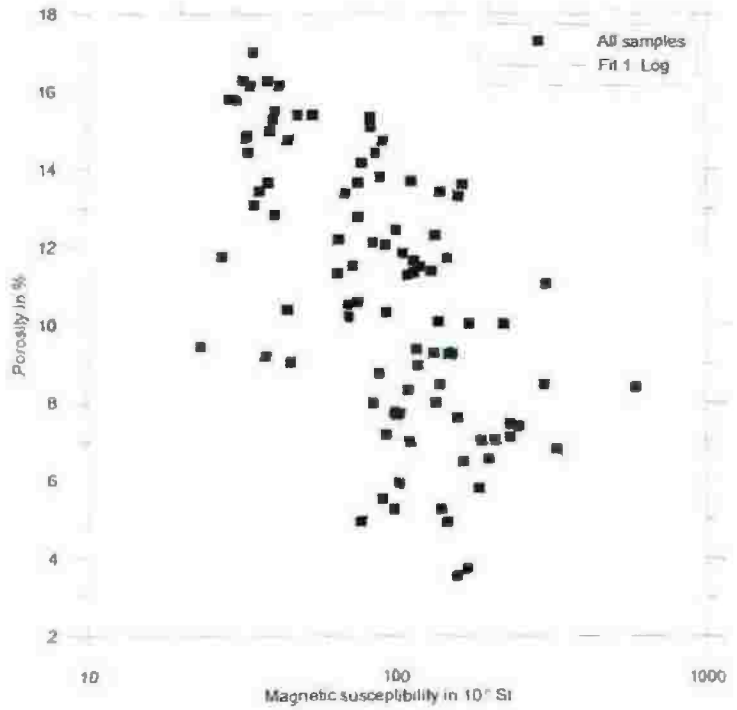

Fig. 4-8 Magnetic susceptibility versus porosity for all samples of the Bahariya Formation. 95 data points are used.

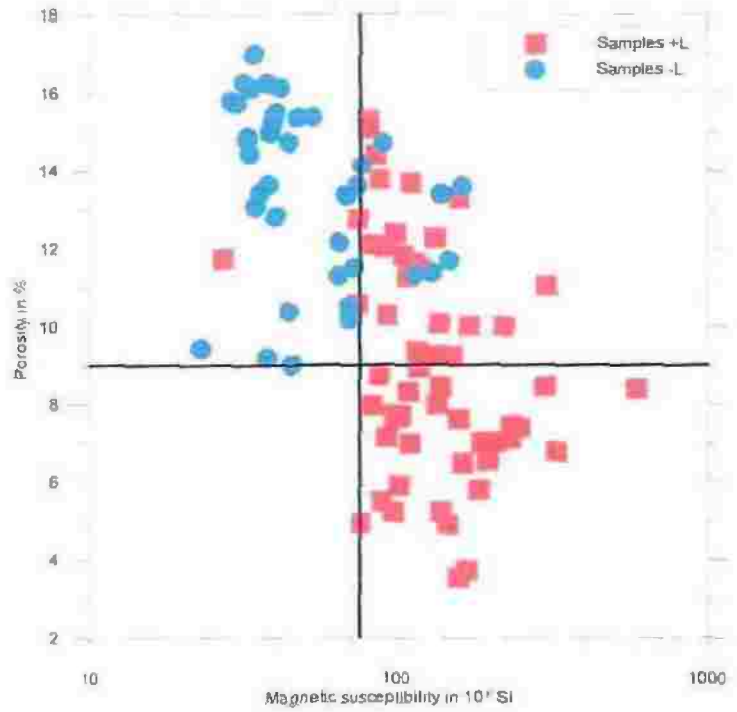

Fig.4-9 Magnetic susceptibility versus porosity for laminated and non-laminated samples of the Bahariya Formation. 57 data points are used for laminated samples and 38 data points are used for non-laminated samples.

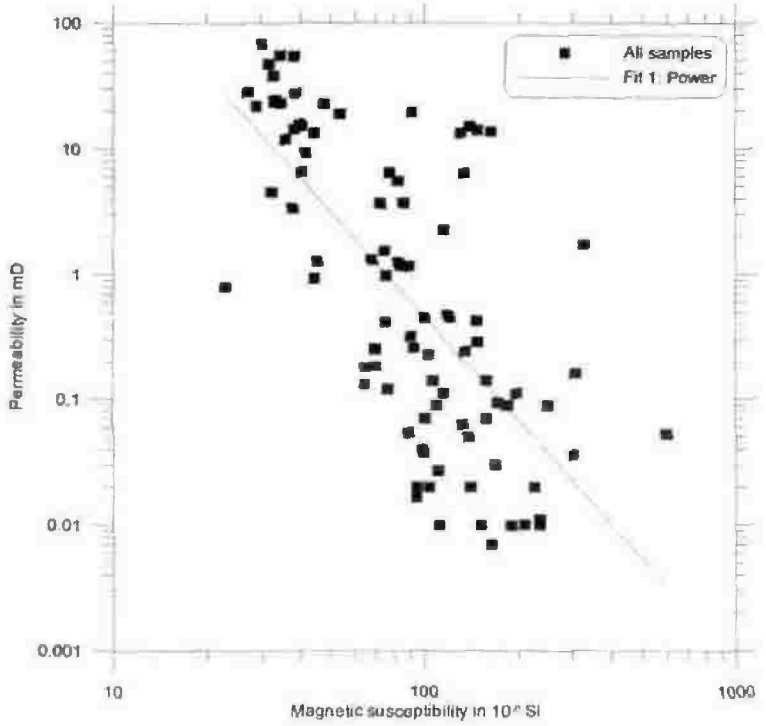

Fig. 4-10 Magnetic susceptibility versus permeability for all samples of the Bahariya Formation. 92 data points are used.

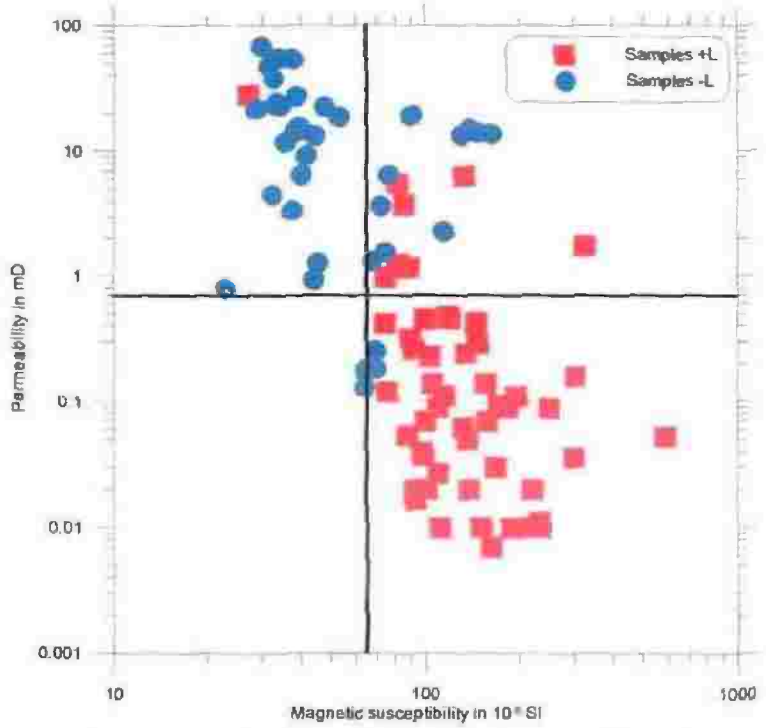

Fig. 4-11 Magnetic susceptibility versus permeability for laminated and non-laminated samples of the Bahariya Formation. 54 data points are used for laminated samples and 38 data points are used for non-laminated samples.

4-6. Internal surface (S_{por}) - permeability relationship

The internal surface (S_{por}) - permeability relationship for the Bahariya samples is shown in Fig. 4-12. The relationship is characterized by a coefficient of determination of 0.53. The internal surface (S_{por}) - permeability relation shows a reverse trend with a general permeability decreases with increasing internal surface (S_{por}). The relationship is controlled by the following power law equation

$$k = 10^{(1.73)} * (S_{por})^{(-1.87)}. \qquad (12)$$

The internal surface (S_{por}) - permeability cross plot for laminated and non-laminated samples is shown in Fig. 4-13. It can be noticed that the laminated samples are characterized by larger internal surface (S_{por}) and lower permeability. The non-laminated samples characterized by smaller internal surface (S_{por}) and high permeability. The data is listed in Tables 2-1, 2, 3 of appendix 1 and 3-1, 2, 3 of appendix 2.

The relationship between internal surface (S_{por}) and porosity for laminated and non-laminated samples is shown in Fig. 4-14. it can be noticed that the upper left quarter contains both non-laminated and laminated samples. The lower right quarter is filled only with laminated samples. The upper right quarter is filed with laminated samples with porosity larger than 8.5 % while the lower left is filled with laminated samples with lower internal surface. Generally, the internal surface (S_{por}) decreases with increasing porosity. The data is listed in Tables 2-1, 2, 3 of appendix 1.

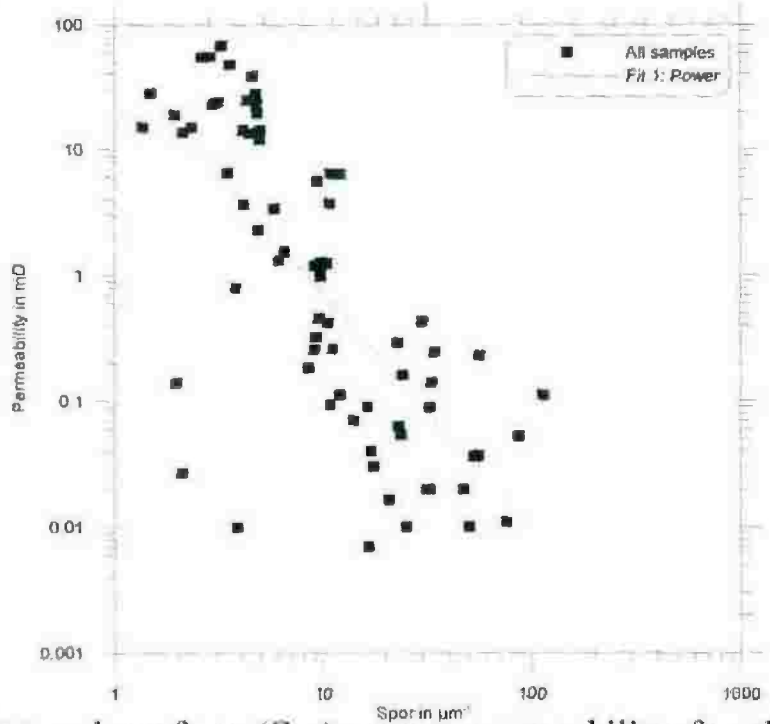

Fig. 4-12 Internal surface (S_{por}) versus permeability for the Bahariya Formation. 72 data points are used.

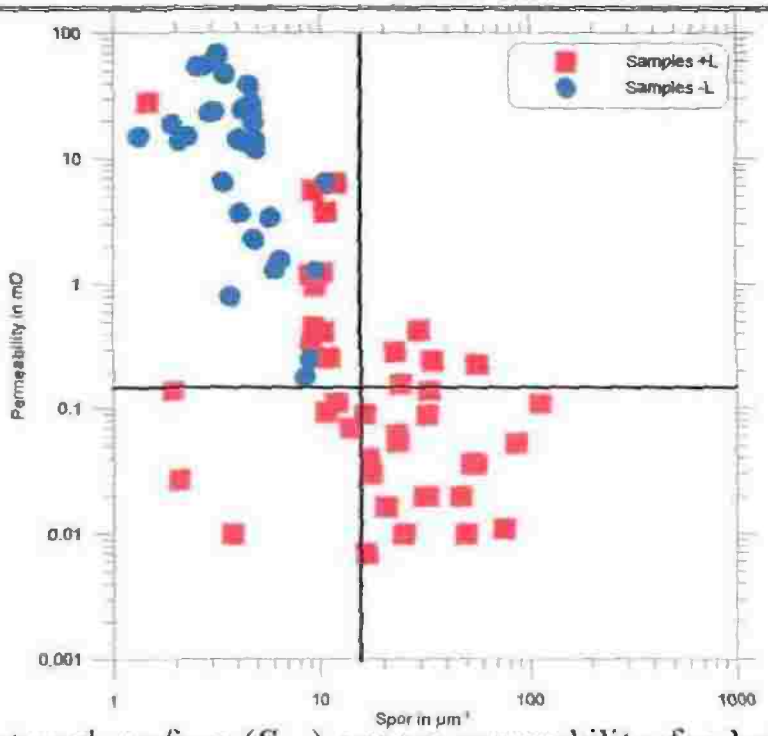

Fig. 4-13 Internal surface (S_{por}) versus permeability for laminated and non-laminated samples of the Bahariya Formation. 42 data points are used for laminated samples and 30 data points are used for non-laminated samples.

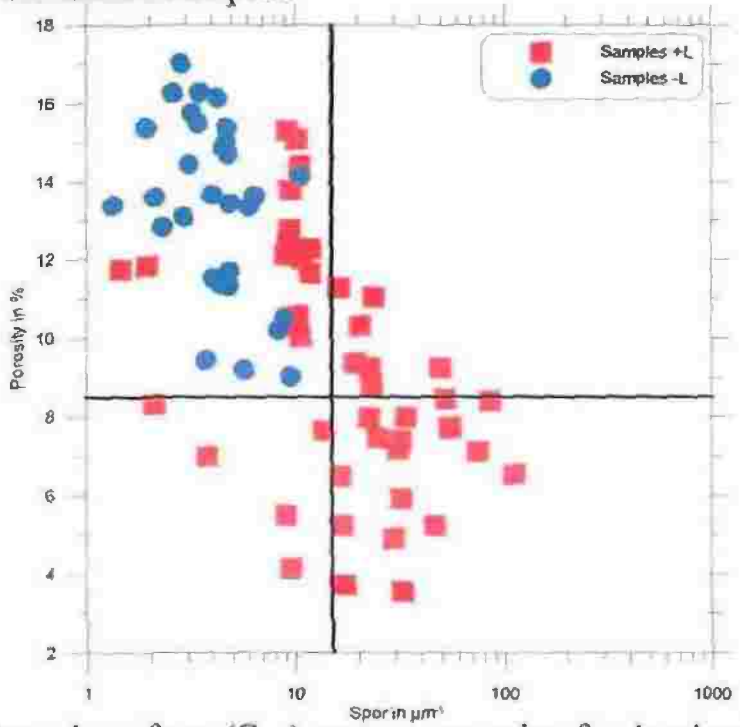

Fig. 4-14 Internal surface (S_{por}) versus porosity for laminated and non-laminated samples of the Bahariya Formation. 45 data points are used for laminated samples and 30 data points are used for non-laminated samples.

4-7. Internal surface (S_{por}) - imaginary part of conductivity relationship

The internal surface (S_{por}) - imaginary part of conductivity relationship for the Bahariya samples has shown highly scattered data points and a very weak coefficient of determination with 0.098. The relationship is shown in Fig. 4-15 and data is listed in Tables 2-2, 3 of appendix 1 and Tables 3-2, 3 of appendix 2. The data points presented in this figure follow the expected positive trend between internal surfaces (S_{por}) and imaginary part of conductivity.

4-8. Permeability - imaginary part of conductivity relationship

The permeability - imaginary part of conductivity relationship for all samples of the Bahariya Formation has shown highly scattered data points and a very weak coefficient of determination of 0.01.

The permeability - imaginary part of conductivity relationships for laminated and non-laminated samples are shown in Fig. 4-16 and data is listed in Tables 3-2, 3 of appendix 2. The data points are highly scattered for non-laminated samples and show a weak coefficient of determination of 0.05. For laminated samples, the cross plot exhibits against the general expectation a positive trend between permeability and imaginary part of conductivity that is characterized by a coefficients of determination of 0.53 and controlled by the equation:

$$k = [10]^{5.66} * [\sigma"]^{4.55} . \qquad (13)$$

4-9. True formation resistivity factor - imaginary part of conductivity relationship

The true formation resistivity factor - imaginary part of conductivity relationship cross plot for the Bahariya samples is shown in Fig. 4-17 and data is listed in Tables 3-2, 3 of appendix 2. The data in these figure shows reverse relations with coefficients of determination for laminated and non-laminated samples of 0.76 and 0.55, respectively. The true formation resistivity factor - imaginary part of conductivity relationships are controlled by the equations:

for laminated samples:

$$\sigma" = [10]^{-0.15} * [F]^{-0.72} , \qquad (14)$$

and for non-laminated samples:

$$\sigma" = [10]^{-0.37} * [F]^{-0.79} . \qquad (15)$$

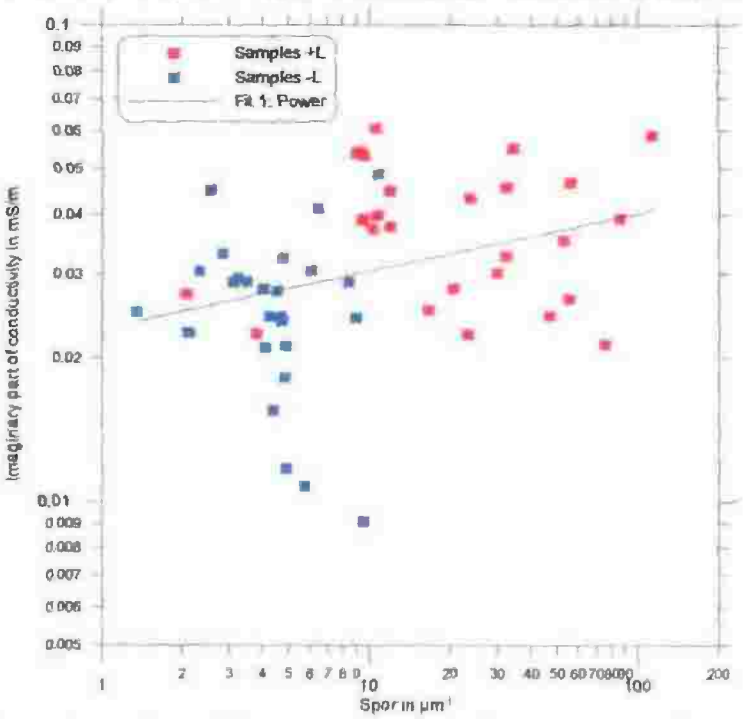

Fig. 4-15 Internal surface (S_{por}) versus imaginary part of conductivity for laminated and non-laminated samples of the Bahariya Formation. 27 data points are used for laminated samples and 26 data points are used for non-laminated samples.

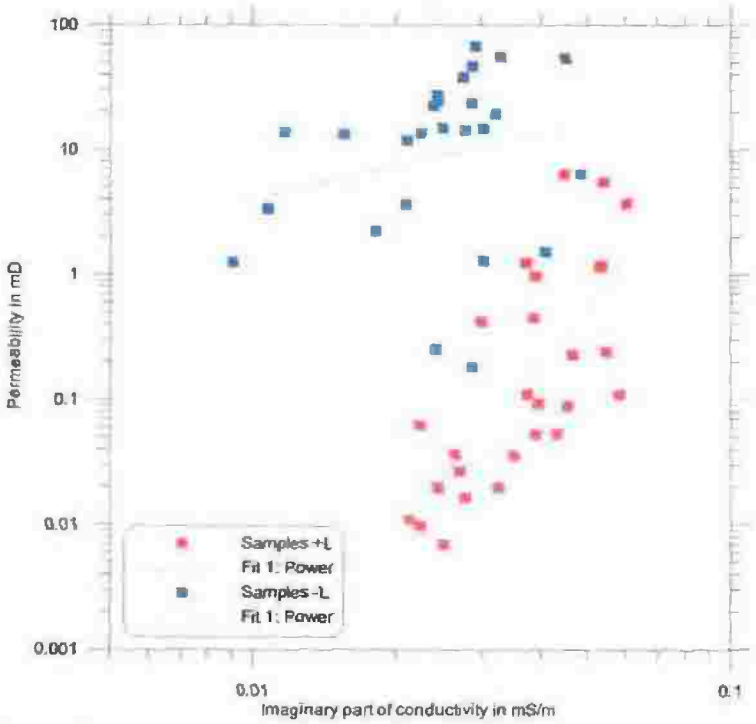

Fig. 4-16 Imaginary part of conductivity versus permeability for laminated and non-laminated samples of the Bahariya Formation. 27 data points are used for laminated samples and 26 data points are used non-laminated samples.

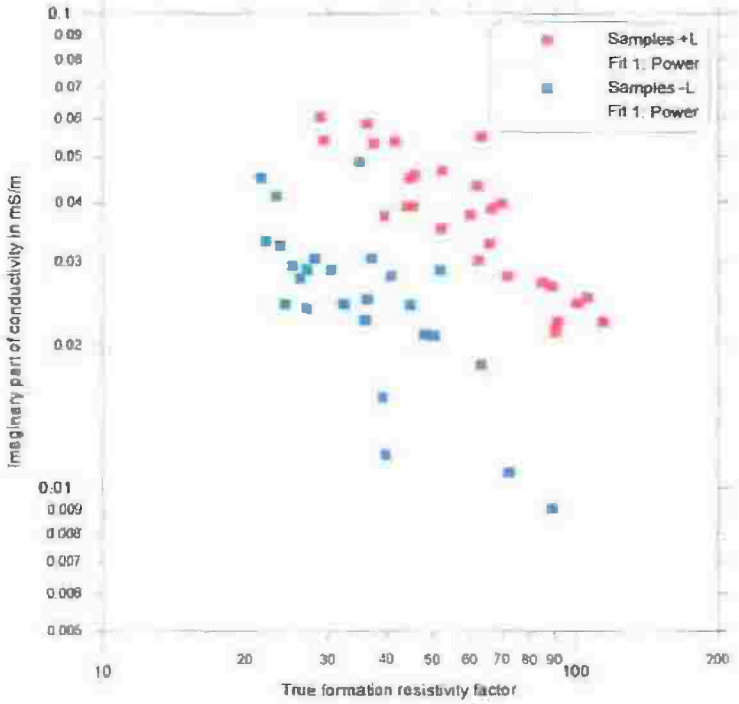

Fig. 4-17 Relationship between true formation resistivity factor and imaginary part of conductivity for laminated and non-laminated samples of the Bahariya Formation. 27 data points are used for laminated samples and 26 data points are used non-laminated samples.

4-10. Porosity - apparent formation resistivity factor relationship

The porosity - apparent formation resistivity factor cross plot for the Bahariya samples is shown in Fig. 4-18, 19. The data in these figures shows reverse relation with coefficients of determination for all, laminated and non-laminated samples of 0.56, 0.34, and 0.79, respectively. The apparent formation resistivity factor - porosity relationships are controlled by the equations:

for all samples:

$$Log\ F_{\backslash} = 2.60 - 0.96\ log\ \Phi, \qquad (16)$$

for laminated samples:

$$Log\ F_{\backslash} = 2.31 - 0.66\ log\ \Phi, \qquad (17)$$

and for non-laminated samples:

$$Log\ F_{\backslash} = 3.61 - 1.86\ log\ \Phi. \qquad (18)$$

Figure 4-19 shows a close relationship for non-laminated samples. Porosity increases with decreasing apparent formation resistivity factor. The resulting factors a and cementation factors m of the general Archie equation are compiled in Table 7.

$$F = \frac{a}{\Phi^m}$$

Table 7: Factors a and cementation factors m from Archie equation.

Bahariya Formation	a	m
All samples	2.60	0.96
Laminated samples	2.31	0.66
Non-laminated samples	3.61	1.86

4-11. Permeability - apparent formation resistivity factor relationship

The apparent formation resistivity factor - permeability cross plot for the Bahariya samples is shown in Fig. 4-20. The data in this figure shows a reverse trend with a permeability increases by decreasing apparent formation resistivity factor. The relation is characterized by a coefficient of determination of 0.56. The apparent formation resistivity factor - permeability relationship is controlled by equation:

$$k = [10]^{(8.07)} * [F']^{(-5.02)}. \quad (19)$$

Figure 4-21 shows the relationship between apparent formation resistivity factor and permeability for laminated and non- laminated samples. The correlation for the non-laminated samples results in a low coefficient of determination of 0.33 but the correlation of the laminated samples is characterized by a coefficient of determination of 0.61. The apparent formation resistivity factor - permeability relations are controlled by the following equations:

for laminated samples:

$$k = [10]^{(6.30)} * [F']^{(-4.25)}, \quad (20)$$

and for non-laminated samples:

$$k = [10]^{(4.73)} * [F']^{(-2.49)}. \quad (21)$$

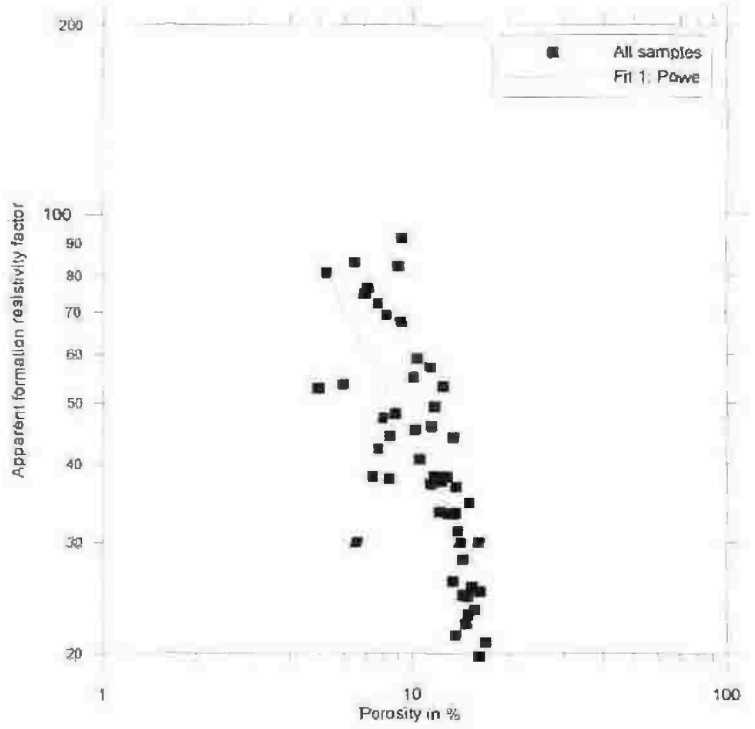

Fig. 4-18 Log porosity versus log apparent formation resistivity factor for all samples of the Bahariya Formation. 53 data points are used.

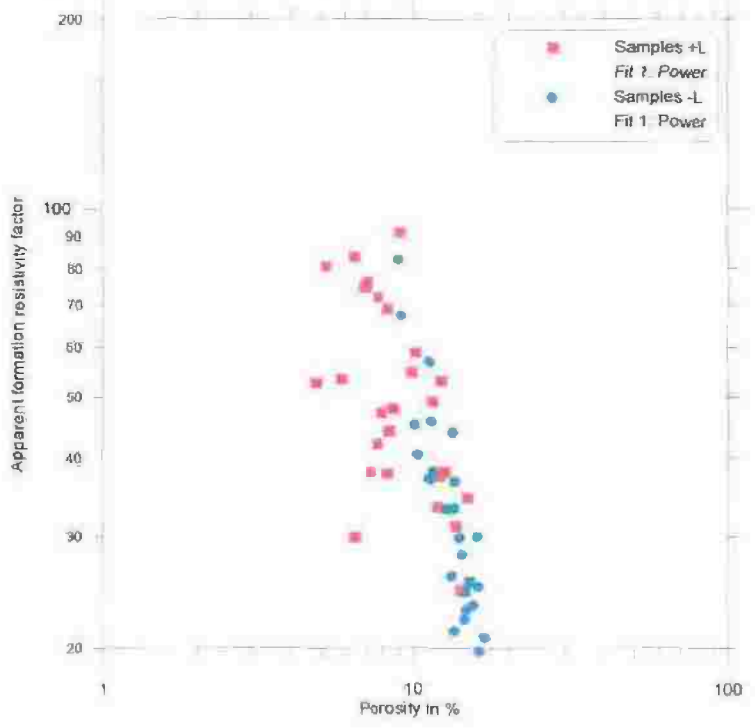

Fig. 4-19 Log porosity versus log apparent formation resistivity factor for laminated and non-laminated samples of the Bahariya Formation. 27 data points are used for laminated samples and 26 data points used are for non-laminated samples.

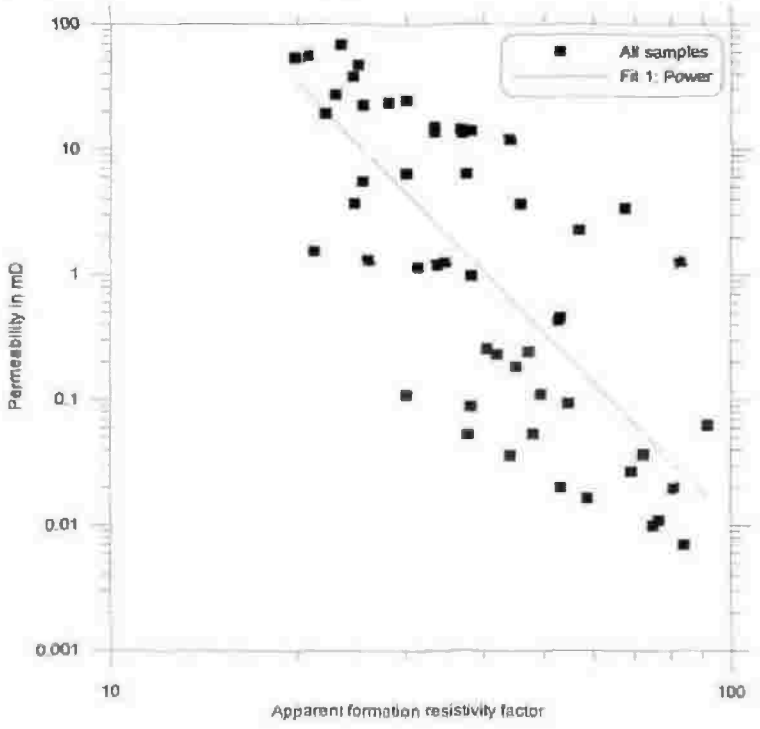

Fig. 4-20 Apparent formation resistivity factor versus permeability for all samples of the Bahariya Formation. 53 data points are used.

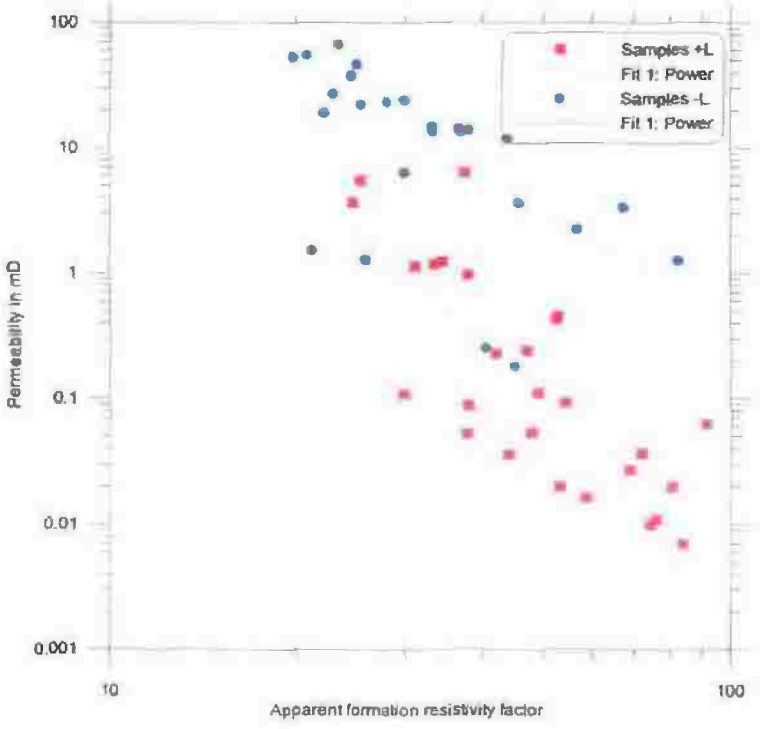

Fig. 4-21 Apparent formation resistivity factor versus log permeability for laminated and non-laminated samples of the Bahariya Formation. 27 data points are used for laminated samples and 26 data points are used for non-laminated samples.

4-12. Porosity - true formation resistivity factor relationship

The porosity - true formation resistivity factor cross plot for the Bahariya samples is shown Figs. 4-22, 23. The data in these figures shows a reverse trend for all samples. The relations are characterized by coefficient of determination for all, laminated and non-laminated samples of 0.59, 0.34, and 0.79, respectively. The consideration of the true instead of the apparent formation resistivity factor results in a slight increase of the coefficients of determination. A correction of the formation factor by the surface conductivity has proved to be reasonable. The true formation resistivity factor - porosity relationships are controlled by the following equations

for all samples:

$$F = [10]^{(2.80)} * [\Phi]^{(-1.08)}, \qquad (22)$$

for laminated samples:

$$F = [10]^{(2.43)} * [\Phi]^{(-0.69)}, \qquad (23)$$

and for non-laminated samples:

$$F = [10]^{(3.68)} * [\Phi]^{(-1.89)}. \qquad (24)$$

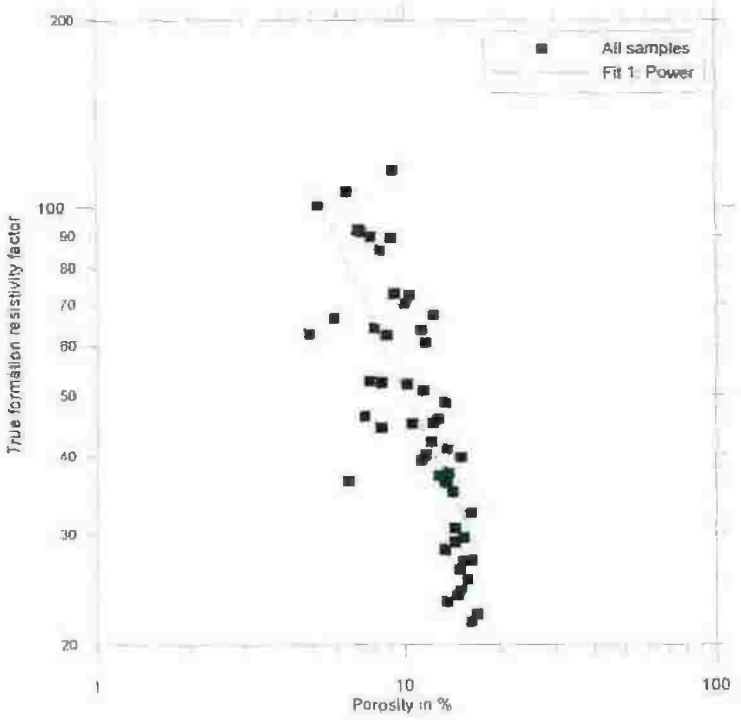

Fig. 4-22 Log porosity versus log true formation resistivity factor for all samples of the Bahariya Formation. 53 data points are used.

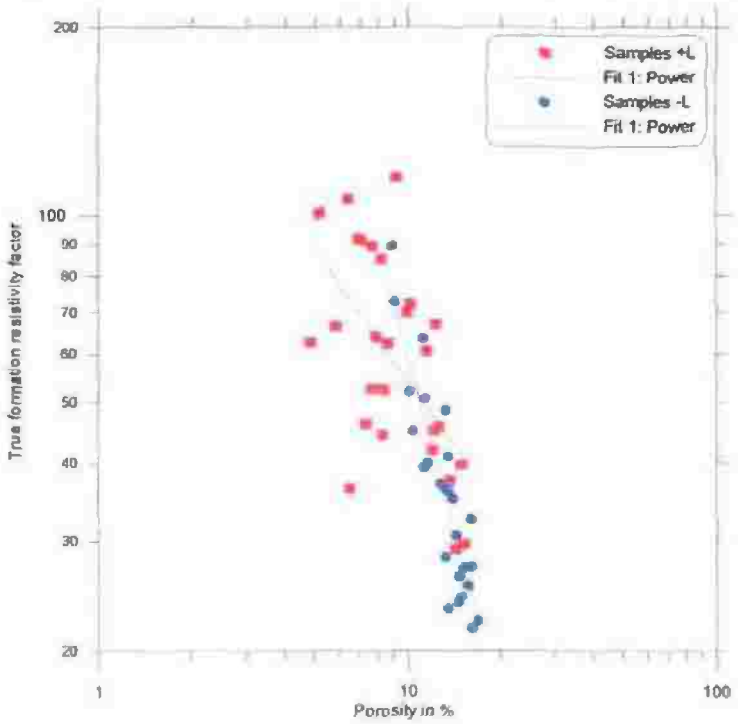

Fig. 4-23 Log porosity versus log true formation resistivity factor for laminated and non-laminated samples of the Bahariya Formation. 27 data points are used for laminated samples and 26 data points are used for non-laminated samples.

4-13. Permeability - true formation resistivity factor relationship

The true formation resistivity factor - permeability cross plot for the Bahariya samples is shown in Fig. 4-24. The data in this figure show a reverse relation for all samples. The relation is characterized by a reliable coefficient of determination of 0.64. The true formation resistivity factor - permeability relationship is controlled by the equation:

$$k = [10]^{(8.15)} * [F]^{(-4.87)}. \quad (25)$$

For non-laminated samples, a coefficient of determination of 0.36 has been determined that is lower than the value for the laminated samples with 0.61. The true formation resistivity factor – permeability relations, which are presented in Fig. 4-25, are controlled by the following equations:

for laminated samples:

$$k = [10]^{(6.30)} * [F]^{(-4.03)}, \quad (26)$$

and for laminated samples:

$$k = [10]^{(4.91)} * [F]^{(-2.55)}. \quad (27)$$

Also in the case of the permeability – true formation resistivity factor relation, a more reliable correlation could be achieved by considering the corrected formation factor (see equation 8 in chapter 3).

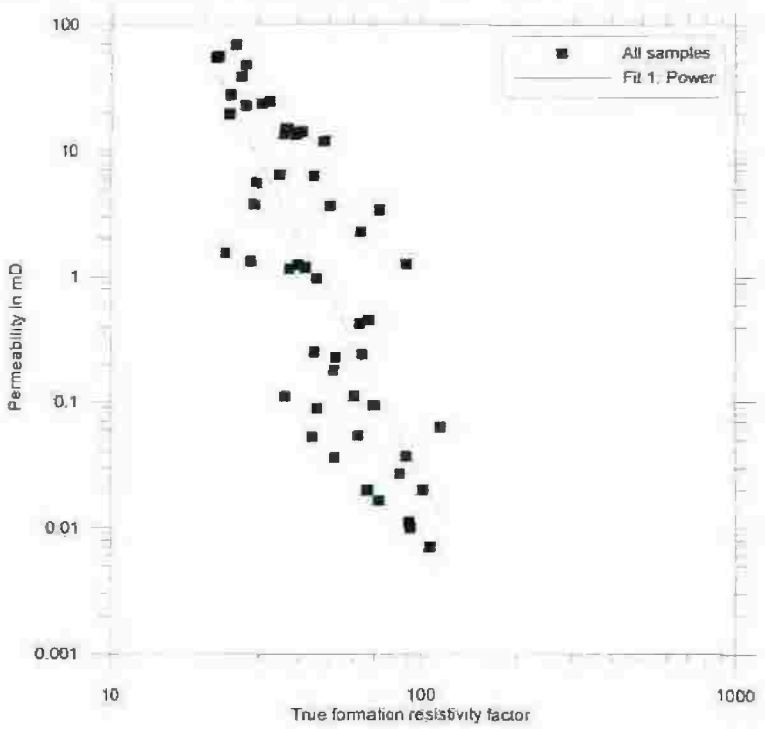

Fig. 4-24 True formation resistivity factor versus log permeability for all samples of the Bahariya Formation. 53 data points are used.

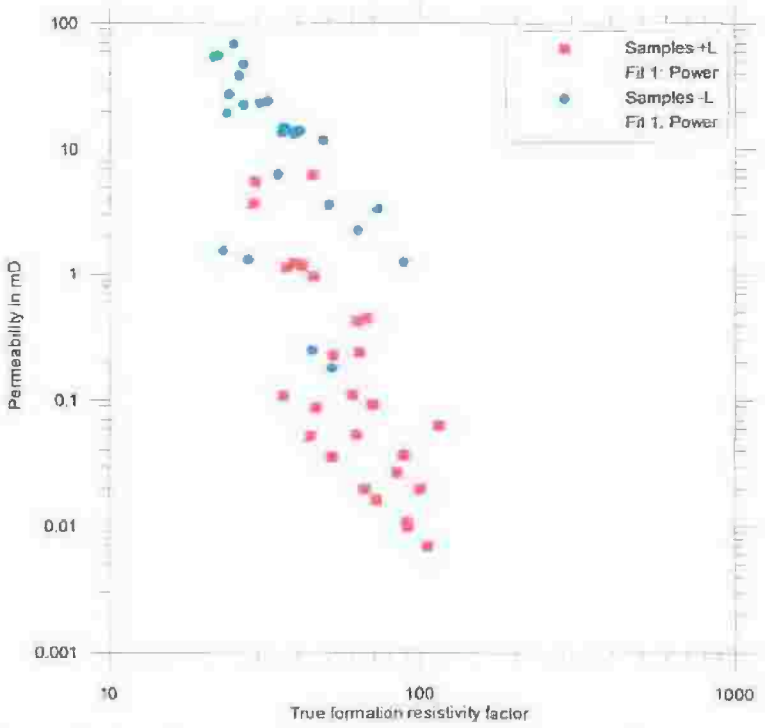

Fig. 4-25 True formation resistivity factor versus log permeability for laminated and non-laminated samples of the Bahariya Formation. 27 data points are used for laminated samples and 26 data points are used for non-laminated samples.

4-14. P-wave velocity - porosity relationship

The p-wave velocity - porosity relationship for the Bahariya samples is shown in Fig. 4-26. The relationship is characterized by a coefficient of determination of 0.43. The p-wave velocity - porosity shows a reverse relation. P-wave velocity decreases with increasing porosity. The relationship is controlled by the following equation:

$$\Phi = 26.99 - 0.005\ Vp. \qquad (28)$$

The p-wave velocity - porosity relationship for laminated and non-laminated samples is shown in Fig. 4-27. This relationship shows a negative trend. The data point are highly scattered for both laminated and non-laminated samples.

P-wave velocity - porosity cross plot for horizontal samples (laminated and non-laminated) is shown in Fig. 4-28. The data points in these figures are characterized by coefficient of determinations for horizontal laminated and non-laminated of 0.57 and 0.45, respectively. The data is listed in Tables 2-1, 2, 3 of appendix 1 and Tables 3-1, 2, 3 of appendix 2.

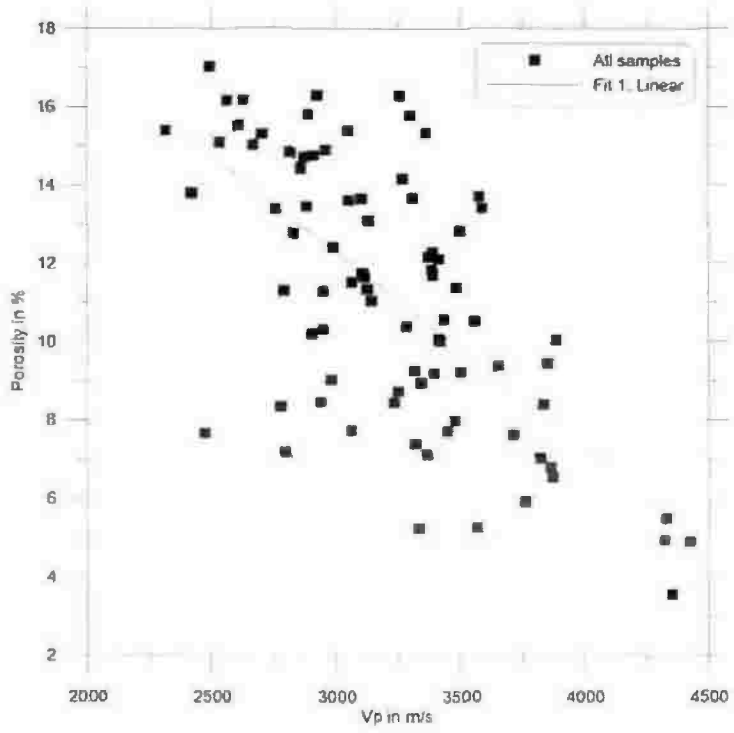

Fig. 4-26 P-wave velocity versus porosity for all samples of the Bahariya Formation. 84 data points are used.

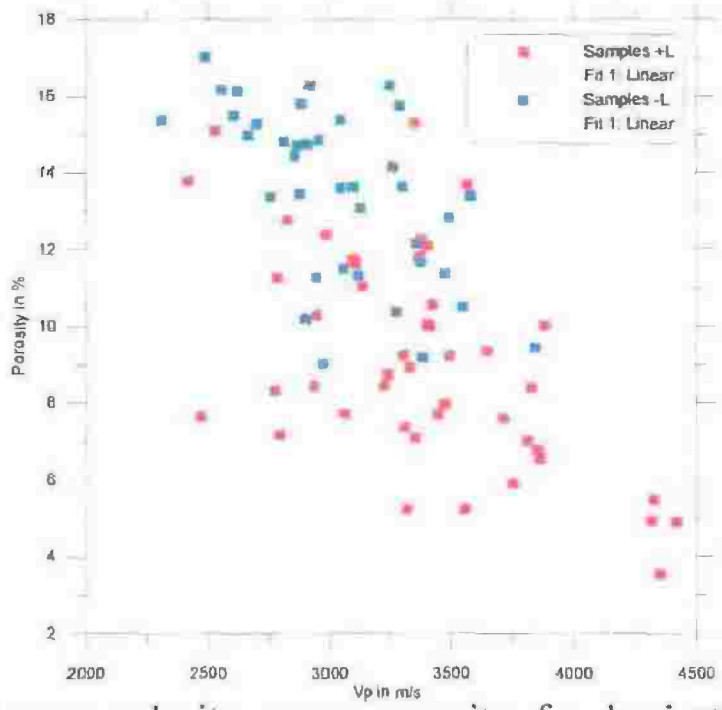

Fig. 4-27 P-wave velocity versus porosity for laminated and non-laminated samples of the Bahariya Formation. 46 data points are used for laminated samples and 38 data points are used for non-laminated samples.

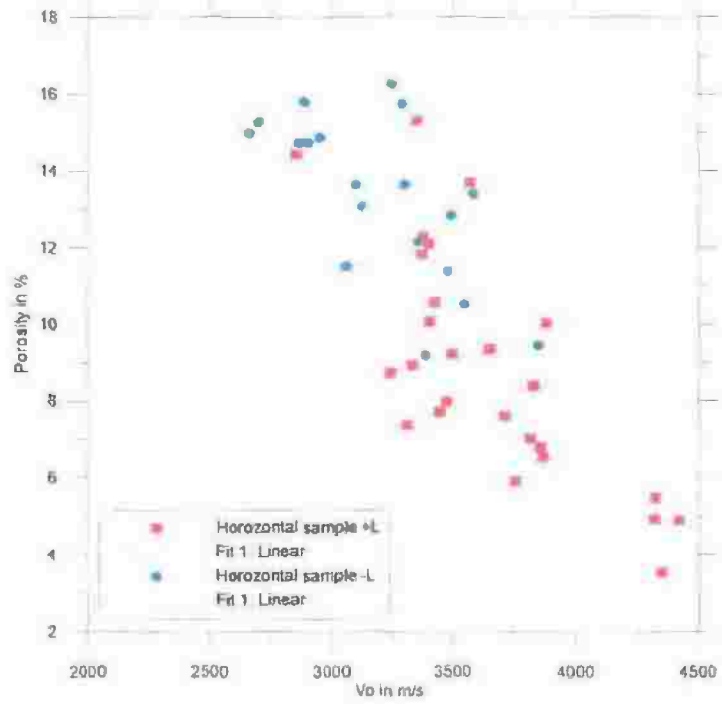

Fig. 4-28 P-wave velocity versus porosity for horizontal (laminated and non-laminated) samples of the Bahariya Formation. 26 data points are used for horizontal laminated samples and 19 data points for horizontal non-laminated samples.

4-15. Anisotropy relationship

The petrophysical investigation of directional parameters has confirmed that in general the laminated samples show a distinct anisotropy. A comparison between the coefficients of anisotropy should reveal whether the anisotropy of resistivity, permeability and seismic p-wave velocity are related to each other.

4-15.1. Relationship between anisotropy of permeability and resistivity

The coefficient of anisotropy of resistivity A_ρ and the coefficient of anisotropy of permeability A_K have been determined by the following equations:

$$A_\rho = \sqrt{\frac{\rho_\perp}{\rho_\parallel}} = \sqrt{\frac{\rho_V}{\rho_H}} \qquad \text{and} \quad A_K = \sqrt[4]{\frac{k_l}{k_t}}, \text{respectively.}$$

The cross plot comparing the coefficient of anisotropy of resistivity and the coefficient of anisotropy of permeability is shown in Fig. 4-29. The diagonal line represents the ideal agreement of the two coefficients. The data points scattering around the ideal line confirm the general trend and show that laminated samples are characterized by a higher degree of anisotropy for both electrical resistivity and permeability. It can be observed that some laminated samples are located at a high distance above the ideal line. This indicates a higher degree of anisotropy in permeability that might be caused by fractures parallel to the bedding plane. Since laminated samples are missing below the diagonal line, it can be concluded that the increase of electrical conduction by fracturing is of minor importance. The data is listed in Tables 4-1, 2, 3 of appendix 3.

4-15.2. Relationship between anisotropy of p-wave velocity and permeability

The anisotropy ratio of seismic p-wave velocity is calculated by the following equation:

$$A_V = \frac{V_H}{V_V}.$$

The cross plot comparing the coefficient of anisotropy of permeability A_K and the anisotropy ratio of seismic p-wave velocity A_V is shown in Fig. 4-30. It can be observed that a larger number of non-laminated samples are located below the diagonal line. The degree of anisotropy stays at low level. The higher degree of anisotropy of the laminated samples is only reflected by anisotropy of permeability while the seismic anisotropy ratio hardly increases.

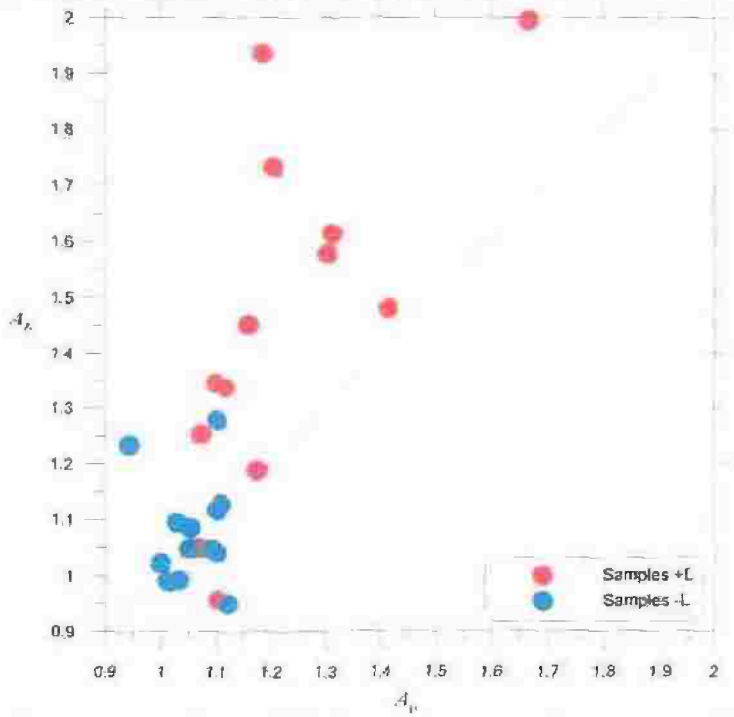

Fig. 4-29 Anisotropy of resistivity versus anisotropy of permeability relationship for laminated and non-laminated samples of the Bahariya Formation. 13 data points are used for laminated samples and 13 data points are used for non-laminated samples.

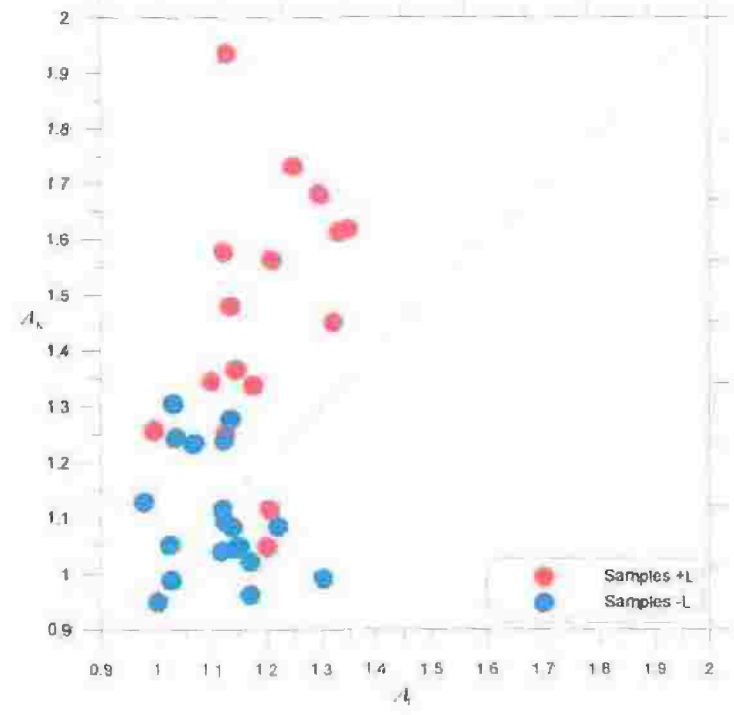

Fig. 4-30 Anisotropy of p-wave velocity versus anisotropy permeability for laminated and non-laminated samples of the Bahariya Formation. 16 data points are used for laminated samples and 19 data points are used for non-laminated samples.

4-15.3. Relationship between anisotropy of resistivity and p-wave velocity

The comparison between anisotropy of electrical resistivity and p-wave velocity which is presented in Figure 4-31 shows a similar behaviour as between coefficient anisotropy of permeability and anisotropy ratio of seismic p-wave velocity. The non-laminated samples are characterized by low anisotropy. The increase of anisotropy for laminated samples is only observed in anisotropy of resistivity. Though there is a slight increase of p-wave velocity observed for laminated samples, the effect of lamination on the anisotropy of seismic velocity can be ignored.

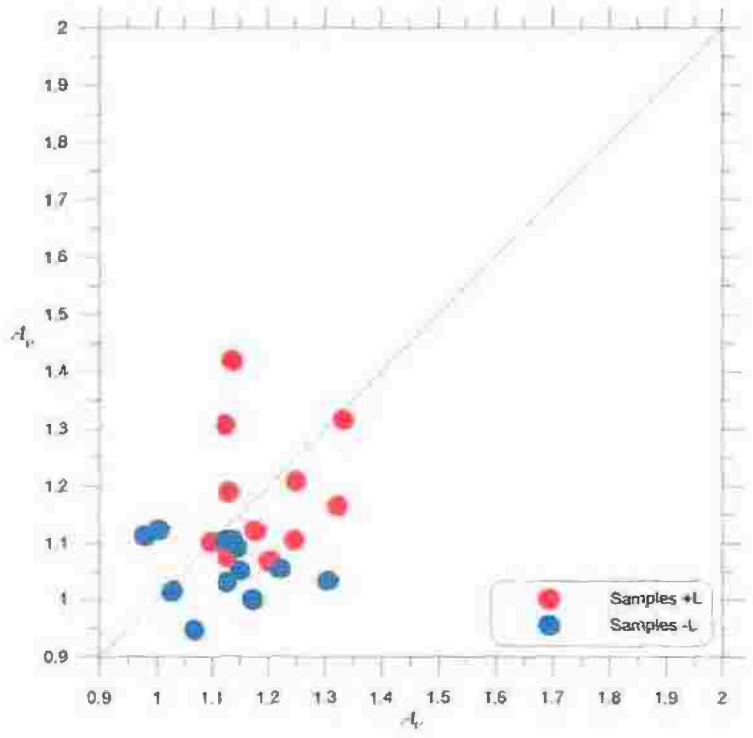

Fig. 4-31 Anisotropy of resistivity versus anisotropy of p-wave velocity for laminated and non-laminated samples of the Bahariya Formation. 11 data points are used for laminated samples and 13 data points are used for non-laminated samples.